Università di Pisa

Low frequency current noise in unstressed/stressed thin oxide metal-oxide-semiconductor capacitors

F. Crupi
Dipartimento di Fisica della Materia e Tecnologie Fisiche Avanzate and INFM,
Università di Messina
Giuseppe Iannaccone
Dipartimento di Ingegneria dell'Informazione: Elettronica, Informatica, Telecomunicazioni,
Università di Pisa
C. Ciofi
Dipartimento di Fisica della Materia e Tecnologie Fisiche Avanzate and INFM,
Università di Messina
Bruno Neri
Dipartimento di Ingegneria dell'Informazione: Elettronica, Informatica, Telecomunicazioni,
Università di Pisa
S. Lombardo
CNR – IMETEM
C. Pace
Dipartimento di Fisica della Materia e Tecnologie Fisiche Avanzate and INFM,
Università di Messina

F. Crupi, G. Iannaccone, C. Ciofi, B. Neri, S. Lombardo, C. Pace, *Low frequency current noise in unstressed/stressed thin oxide metal-oxide-semiconductor capacitors*, Solid-state Electronics, **46**, pp.1807-1813 (2002).

PERGAMON

Solid-State Electronics 46 (2002) 1807–1813

SOLID-STATE ELECTRONICS

www.elsevier.com/locate/sse

Low frequency current noise in unstressed/stressed thin oxide metal-oxide-semiconductor capacitors

F. Crupi [a,*], G. Iannaccone [b], C. Ciofi [a], B. Neri [b], S. Lombardo [c], C. Pace [a]

[a] *Dipartimento di Fisica della Materia e Tecnologie Fisiche Avanzate and INFM, Salita Sperone 31, I-98166 Messina, Italy*
[b] *Dipartimento di Ingegneria della Informazione, Via Diotisalvi 2, I-56126 Pisa, Italy*
[c] *CNR-IMETEM, Stradale Primosole, 50, I-95121 Catania, Italy*

Abstract

In this work we investigate the low frequency current noise in metal-oxide-semiconductor structures biased with a constant voltage in different oxide degradation stages. We report $1/f$ noise in fresh oxides with an anomalous current dependence that is quite similar to what has been reported in the direct tunneling regime. A higher flicker noise level is observed after stressing the oxide. Both observations are ascribed to the presence of an additional tunneling component assisted by native or stress-induced oxide traps. A further increase of the low frequency current noise is observed after the oxide breakdown (BD). It is shown that in the quantum point contact case single fluctuators, probably consisting of electron traps inside the oxide, can be resolved, whereas the current noise at the thermal BD presents a $1/f$ spectrum, due to the effects of ensemble averaging between many of these fluctuators.
© 2002 Elsevier Science Ltd. All rights reserved.

Keywords: MOS devices; Tunneling current; Noise; Quantum point contact

1. Introduction

Much effort has been dedicated to the study of the charge trapping and transport mechanisms in the SiO_2 film in metal-oxide-semiconductor (MOS) structures. The interest for this subject is twofold. On the one hand, the presence of trapped charge and conduction currents in the oxide represents the main reliability issue in modern CMOS ULSI circuits. On the other hand, there are circuits, such as nonvolatile memories, that use the conduction mechanisms through the oxide for their normal operation. Different tunneling mechanisms have been identified in unstressed and stressed oxide: Fowler–Nordheim (FN) tunneling [1], direct tunneling [2], tunneling assisted by native or stress-induced oxide traps [3,4] and tunneling involving the Si–SiO_2 interface states [5,6].

Recently also the conduction through a broken oxide has gained much attention. This interest is justified by the observation that in thinner oxides the oxide breakdown (BD) does not necessary coincide with the circuit failure, due to a decrease in the post-BD conductance [7,8]. In 1998, Suné et al. first suggested that the oxide hard-BD (HBD) behaves as a quantum point contact (QPC) [9]. Their thesis was mainly supported by the observation that the conductance of a broken down oxide exhibits a plateau of the order of the quantum conductance, $2e^2/h$, where h is the Planck constant and e is the elementary charge. Lower conductance values observed in broken down oxides have been ascribed to a different conduction mechanism, the so-called soft-BD [10], whereas higher conductance values have been attributed to the formation of several BD spots [9] and/or to the lateral propagation of the BD region [11].

Most of the characterization regarding the charge trapping and transport in MOS structures before and after the oxide BD is based on the measurements of the dc component of the current and on C–V measurements. On the other hand, it is well known that the current

* Corresponding author. Tel.: +39-90-6765648; fax: +39-90-391382.
E-mail address: fcrupi@ingegneria.unime.it (F. Crupi).

0038-1101/02/$ - see front matter © 2002 Elsevier Science Ltd. All rights reserved.
PII: S0038-1101(02)00153-3

noise is a sensitive probe of the interaction of the charge carriers with defects or other charge carriers [12]. In this work we investigate the low frequency current noise in MOS structures at different oxide degradation stages. Section 3 is dedicated to the case of unstressed and stressed oxide before the BD, whereas in Section 4 we focus on the low frequency current noise after the oxide BD.

2. Experimental

MOS capacitors were prepared on (1 0 0) oriented n^+ silicon substrates with an n^- epitaxy (5×10^{15} cm^{-3}). The 6 nm thick gate oxide was grown in O_2 atmosphere. Two different sample areas have been used, $A_S = 10^{-4}$ cm^2 and $A_L = 1.225 \times 10^{-3}$ cm^2. The polycrystalline silicon was n^+ doped by using a chemical diffusion source of $POCl_3$. Finally the devices were packaged in metal frames.

The devices were stressed at room temperature by injecting electrons from the substrate using a current limited constant voltage stress [13] with 7.8 V gate voltage and with two different current compliance levels, 100 μA and 10 mA. The current noise has been evaluated in three different stages: before stressing, after stressing and before oxide BD, at oxide BD. In order to associate the measured power spectral density (PSD) of the current noise measured at constant voltage to a fixed dc current level, we checked that the change of the level of the dc current during a single measurement was smaller than 1% of the corresponding average value. The stress and I–V measurements have been performed with a Semiconductor Parameter Analyzer HP4155B, whereas the noise measurements have been realized by means of a purposely designed measurement system, essentially consisting of a low noise differential transimpedance amplifier including a biasing stage and a personal computer based spectrum analyzer.

3. Noise before breakdown

The typical current noise PSD in a 6 nm fresh oxide is shown in Fig. 1. Two different components are clearly distinguishable: at lower frequencies a flicker component is observed, while at higher frequencies a shot component is predominant [14,15]. Fig. 2 reports the PSD of the flicker noise, S_i, in the band between 0.1 and 1 Hz measured at different dc current levels, I_{DC}, in a fresh 6 nm oxide with an area of $A_S = 10^{-4}$ cm^2. The electric field range has been chosen sufficiently high so that the current spectrum level was distinguishable from the background instrumentation noise spectrum and sufficiently low so that the FN current was essentially steady state. In each case we found a $1/f^{\beta}$ power law form with

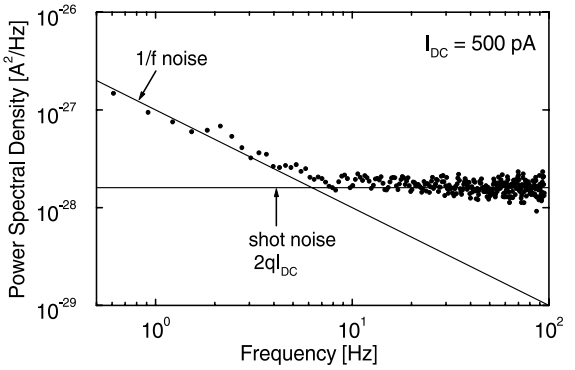

Fig. 1. PSD of the current noise measured in a 6 nm fresh oxide. Two different noise components can be distinguished: a $1/f$ noise component dominant at lower frequencies and a shot noise component dominant at higher frequencies.

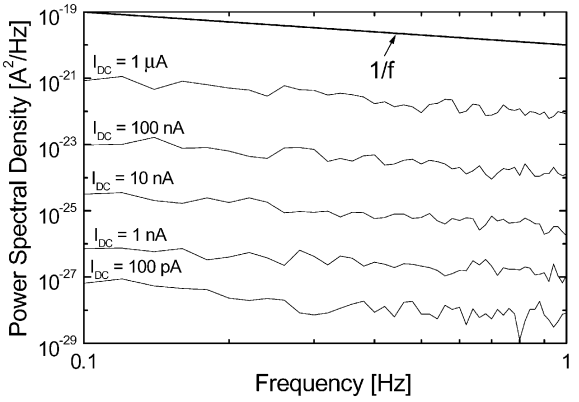

Fig. 2. PSD of the flicker noise component as a function of the frequency measured in a 6 nm fresh oxide at different dc current levels. A clear $1/f$ behavior is observed in all cases.

β very close to 1, in agreement with other works [16,17]. In order to compare the spectra measured at different dc currents, we evaluated the following normalized noise power:

$$P_n = \int_{0.1\ \mathrm{Hz}}^{1\ \mathrm{Hz}} \frac{S_i(f)}{I_{DC}^2}\,df \tag{1}$$

The values of P_n as a function of the dc current density is shown in Fig. 3. In the same figure we plot the P_n measured in a larger area $A_L = 1.225 \times 10^{-3}$ cm^2 oxide multiplied for the area ratio A_L/A_S. At higher dc current densities, the values of P_n result quite independent of the dc current density, in agreement with the data reported in [17], whereas at lower dc current densities, the values of P_n rise, as reported by Alers et al. in the case of direct tunneling regime [18,19].

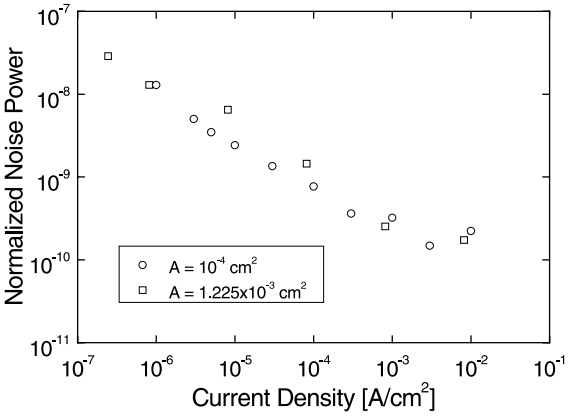

Fig. 3. Power of the current flicker noise in the band between 0.1 and 1 Hz normalized with respect to the square of the dc current as a function of the dc current density measured in a 6 nm fresh oxide. The data obtained in the larger area sample have been multiplied by the ratio between the larger and the smaller area. The normalized noise power results quite constant at higher current densities and increases at lower current densities.

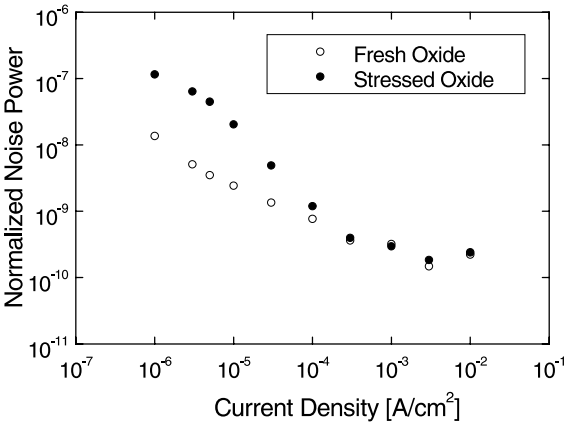

Fig. 4. Power of the current flicker noise in the band between 0.1 and 1 Hz normalized with respect to the square of the dc current as a function of the dc current density measured in a 6 nm oxide before and after the application of a high field stress. After stressing the oxide the flicker noise power increases at low fields where also the dc current level increases (SILC).

After the application of a high field stress, a stress-induced leakage current (SILC) at low voltage is observed. The PSD of the current noise still consists of a flicker component dominant at lower frequencies and a white component dominant at higher frequencies. The shot noise component after stress results partially suppressed with respect to the full shot noise value observed in the FN regime, as reported in previous works [14,15]. An opposite trend is observed for the flicker component. We evaluated the normalized noise power, P_n, in the band between 0.1 and 1 Hz before and after the application of a high field stress. The obtained values are plotted in Fig. 4. At higher dc current densities, where the FN tunneling is always the dominant transport mechanism, the P_n values after the stress result quite constant and no appreciable change is observed with respect to the values measured before the stress. This means that the mechanism that is responsible for $1/f$ noise in FN tunneling current is not significantly affected by the electrical field stress. At lower dc current densities, when there is a significant contribution of SILCs, a large increase of the P_n values after the stress is observed.

There are few mechanisms that may be responsible for this behavior. Alers et al. [19] proposed a model in which the low frequency noise in the SILC regime is due to the slow modulation of the activity of traps assisting the SILCs. This model would be able to explain the increase of $1/f$ noise after stress at low current densities, and also the fact that P_n after stress tends to saturate to a constant (high) level decreasing the current densities. According to the model proposed in [19], the increase of P_n at low current densities before stress may be due to traps assisting the SILCs already present in the fresh oxide, that give a small contribution to the current but significantly increase the noise power. Note that the presence of trap-assisted-tunneling in fresh oxides is also confirmed by the comparison between the measured J–V curve with that obtained by means of a 1-D Poisson–Schrodinger simulator (Fig. 5). As the simulator only evaluates the pure tunneling component, the deviation between the two data sets at low fields indicates a tunneling component assisted by native traps, in agreement with other works [4,20]. However, such a model does not explain the $1/f$ noise observed at high current densities,

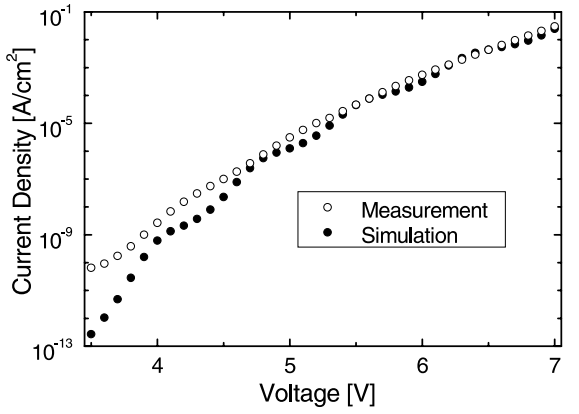

Fig. 5. Comparison of the J–V characteristics measured and simulated for a 6 nm fresh oxide. A deviation between the two curves is observed at low fields, where an additional current component has been measured.

which cannot be due to the stress-induced traps, because it practically does not change after electric stress.

Another possible mechanism for $1/f$ noise in SILCs and FN currents is barrier modulation due to charging and discharging of slow traps in the oxide. Such traps, with capture and emission times of the order of seconds, would be different from those contributing to trap-assisted-tunneling. For simplicity, we would call the former "slow" traps and the latter "fast" traps. When a slow trap is charged, it affects both FN tunneling and trap-assisted-tunneling in the vicinity of the trap itself. However, trap-assisted-tunneling is much more affected by the presence of charged slow traps than FN tunneling. The situation is sketched in Fig. 6: when the slow trap is charged, the barrier for FN tunneling increases. On the other hand, a charged slow trap also increases the energy of a nearby fast trap, so that trap-assisted-tunneling is reduced for two concurrent reasons: the increase of the tunneling barrier, and the increased energy of the trap, which makes hopping through that trap energetically disadvantaged. The same reasoning apply if we consider fast traps with a finite distribution in energy. When a nearby slow trap is charged, lower energy fast traps (indicated with letter A in Fig. 6b) are effectively replaced by much higher energy traps (indicated with letter B in Fig. 6b), through which tunneling is highly unfavored. Since P_n at large current densities does not change after stress, one should assume that the concentration of slow traps is not affected by electric stress, and that such traps are already present in the fresh oxide. Further experiments, and quantitative models, are needed to determine the mechanism actually responsible for $1/f$ noise before and after stress.

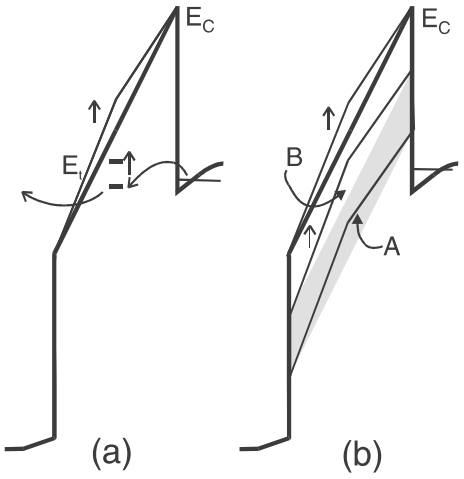

Fig. 6. Sketch of the conduction band in the oxide when the slow trap is discharged (thick line) and charged (thin line). In (a) a fast trap is sketched whose energy increases because of the charged slow trap, while in (b) a region in energy and space in which fast traps are distributed (dashed region) is modified as shown with thin lines when a slow trap is charged. As a result, region "A" is effectively replaced by region "B", at a much larger energy.

4. Noise at breakdown

In Fig. 7 we report the post-BD conductance, normalized with respect to the quantum conductance, $2e^2/h$, as a function of the voltage for two different values of the current compliance used during the stress. Both curves present an initial increase up to 1 V and a successive plateau. Two different HBD modes can be clearly distinguished: for the lower current compliance, the post-HBD conductance results close to the quantum conductance, that is a feature of a Fermi-length size constriction (QPC-HBD) [21], whereas for the higher current compliance, the post-HBD conductance results higher by a factor $\approx$10, thus indicating a larger BD region, due to stronger thermal effects (thermal HBD).

In both cases, we have observed a high increase not only of the dc component of the current but also of the low frequency noise compared with the case of a not broken oxide, as a consequence of the localized nature of the HBD. After the QPC-HBD occurrence, we always observed two-level or multilevel random telegraph signal (RTS) in the current through the BD contact. The individual fluctuators responsible for this phenomenon can be ascribed to the capture–emission process of a single electron in a defect site inside the oxide close to the HBD spot. A typical example of two-level fluctuations (TLF) is reported in Fig. 8. The high value of the TLF relative amplitude, about 20% at all bias, indicates

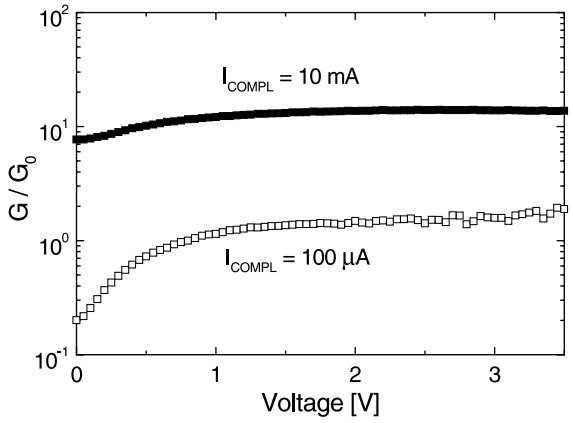

Fig. 7. Post-BD conductance G normalized with respect to the quantum conductance, $G_0 = 2e^2/h$, as a function of the voltage for two different levels of the current compliance used during the constant voltage stress. Two different HBD modes can be clearly distinguished.

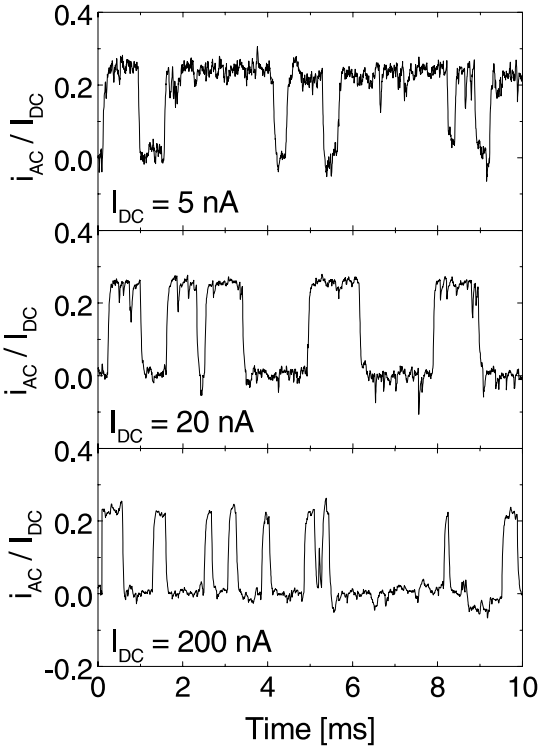

Fig. 8. Time evolution of the ac current component i_{AC} normalized with respect to the dc current component I_{DC} for different values of the dc current after the QPC-HBD. TLF are observed.

that the corresponding defect is completely bathed by the electron flux through the HBD spot. In Fig. 9 we plot the average time in which the current is in the high state, capture time τ_c, and the average time in which the current is in the low state, emission time τ_e, as a function

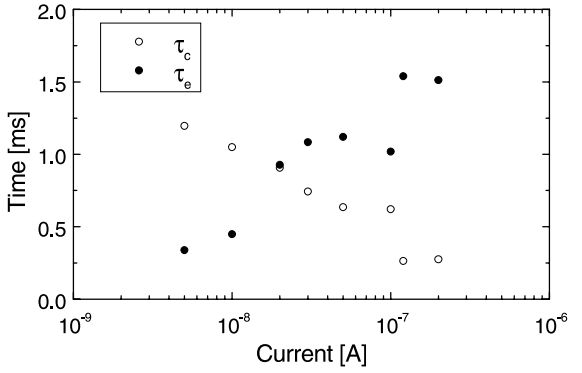

Fig. 9. Capture and emission time of a two-level RTS as a function of the dc current component measured in the same sample of Fig. 8. Each point has been obtained by averaging over more than 200 transitions. An opposite trend is observed for the two time constants.

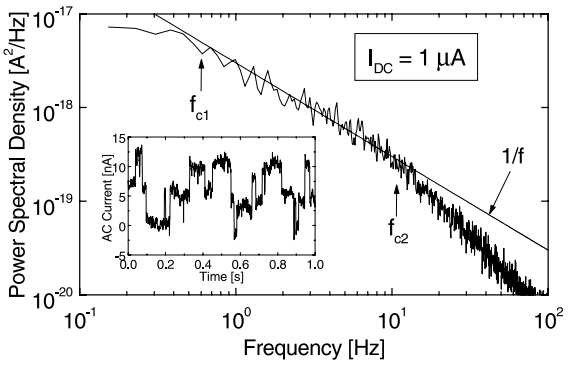

Fig. 10. PSD of the current noise measured in a QPC-HBD. The corresponding time evolution is reported in the inset. A $1/f$ behavior is observed in the bandwidth between the frequency corners of the two RTSs.

of the dc component of the current. The current dependence of the TLF constant times indicates a strong interaction between the defect and the electron flux through the HBD spot. The decrease of τ_c with the current can be explained by the corresponding increase of the electron flux, whereas the increase of τ_e with the current can be a consequence of the lower number of states available for the conduction. In Fig. 10 we plot the PSD of the current noise through the QPC-HBD spot measured in another sample. As shown in the inset, in this case two RTSs with different corner frequencies, $f_{c1} \approx 1$ Hz and $f_{c2} \approx 10$ Hz, are active in the measurement bandwidth. It can be observed that in the bandwidth between f_{c1} and f_{c2} the PSD shows a $1/f$ behavior as a result of the overlapping of the two Lorentzian spectra. After the occurrence of the thermal HBD, the low frequency current noise presents a $1/f$ spectrum as shown in Fig. 11. In this case, we never observed RTS

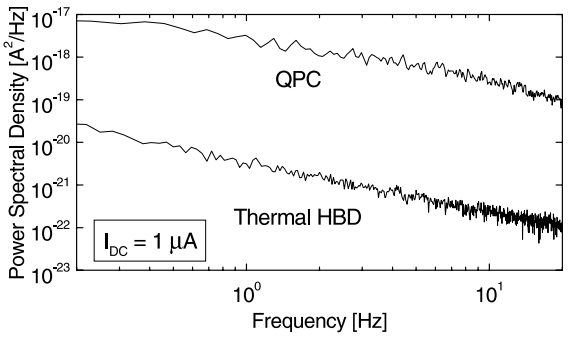

Fig. 11. Comparison of the low frequency noise measured in a QPC-HBD and in a thermal HBD at the same dc current level. Noise after thermal HBD shows a $1/f$ behavior and a lower magnitude comparing to the case of the QPC-HBD.

noise and the level of the low frequency current noise was a few orders of magnitude lower than the QPC-HBD case. Both differences can be ascribed to the larger area A of the thermal HBD and, therefore, to the higher number of active fluctuators. In fact, it is well known that the superposition of a sufficiently high number of RTSs generates a $1/f$ spectrum proportional to $1/A$.

It is worth noting that after the HBD occurrence, there is a local damage not only of the oxide, but also of the silicon structure. In particular, in a previous work, we have observed in thicker oxides a large density of threading dislocations in the silicon substrate after HBD [22], thus we can not exclude that the electron trapping–detrapping process occurs in the silicon.

5. Conclusions

In this paper we have analyzed low frequency current noise in a MOS structure with a 6 nm oxide at different oxide degradation stages.

In fresh oxides, the low frequency current noise shows a $1/f$ noise behavior with an anomalous current dependence. A higher flicker noise level is observed in the SILCs. A model based on the barrier modulation due to charging and discharging of slow traps in the oxide has been proposed for explaining the experimental data. Further experiments, and quantitative models, are strongly required to clarify the origin of the $1/f$ noise before and after stress.

Depending on the current compliance used during a constant voltage stress, two different HBD modes have been observed, characterized by conductance values close to the quantum conductance (QPC) or significantly higher (thermal BD). It is shown that in the QPC case, the low frequency noise is characterized by a few Lorentzian components, due to individual fluctuators, probably consisting of electron traps inside the oxide. After the thermal HBD, the low frequency current noise shows a $1/f$ behavior and lower magnitude, as a consequence of the higher number of fluctuators, that are present in the larger area BD region.

Acknowledgements

This work has been supported by the Italian National Research Council (CNR) through the Finalized Project MADESSII.

References

[1] Fowler RH, Nordheim L. Electron emission in intense electric fields. Proc R Soc London Ser A 1928;119:173–81.

[2] Schuegraf KF, King CC, Hu C. Ultra-thin silicon dioxide leakage current and scaling limit. VLSI Symp 1992: 18–9.

[3] Moazzami R, Hu C. Stress-induced current in thin silicon dioxide films. IEDM Tech Dig 1992:139–42.

[4] Ghetti A, Sangiorgi E, Sorsch TW, Kizilyalli I. The role of native traps on the tunneling characteristics of ultra thin (1.5–3 nm) oxides. Microelectron Eng 1999;48:31–4.

[5] Nicollian PE, Rodder M, Grider DT, Chen P, Wallace RM, Hattangady SV. Low voltage stress-induced-leakage-current in ultrathin gate oxides. Proc Int Reliab Phys Symp 1999:400.

[6] Ghetti A, Sangiorgi E, Bude J, Sorsch TW, Weber G. Low voltage tunneling in ultra-thin oxides: a monitor for interface states and degradation. IEDM Tech Dig 1999: 731.

[7] Weir BE, Silverman PJ, Monroe D, Krisch KS, Alam MA, Alers GB, et al. Ultra-thin gate dielectrics: they break down, but do they fail? IEDM Tech Dig 1997:73.

[8] Kaczer B, Degraeve R, Groeseneken G, Rasras M, Kubicek S, Vandamme E, et al. Impact of MOSFET oxide breakdown on digital circuit operation and reliability. IEDM Tech Dig 2000:553.

[9] Suné J, Miranda E, Nafria M, Aymerich X. Point contact conduction at the oxide breakdown of MOS devices. IEDM Tech Dig 1998:191.

[10] Crupi F, Degraeve R, Groeseneken G, Nigam T, Maes HE. On the properties of the gate and substrate current after soft-breakdown in ultra-thin oxide layers. Trans Electron Dev 1998;45(11):2329–34.

[11] Lombardo S, La Magna A, Spinella C, Gerardi C, Crupi F. Degradation and hard breakdown transient of thin gate oxides in metal-SiO_2-Si capacitors: dependence on oxide thickness. J Appl Phys 1999;86:6382–91.

[12] Kirton MJ, Uren MJ. Noise in solid-state microstructures: A new perspective on individual defects, interface states and low-frequency ($1/f$) noise. Adv Phys 1989;38:367–468.

[13] Linder BP, Stathis JH, Wachnik RA, Wu E, Cohen SA, Ray A, et al. Gate oxide breakdown under current limited constant voltage stress. VLSI Symp 2000:214–5.

[14] Crupi F, Iannaccone G, Neri B, Ciofi C, Lombardo S. Shot noise partial suppression in the SILC regime. Microelectron Reliab 2000;40:1605–8.

[15] Iannaccone G, Crupi F, Neri B, Lombardo S. Suppressed shot noise in trap-assisted tunneling of metal-oxide-semiconductor capacitors. Appl Phys Lett 2000;77(18):2876–8.

[16] Neri B, Olivo P, Riccò B. Low-frequency noise in silicon-gate metal-oxide-silicon capacitors before oxide breakdown. Appl Phys Lett 1987;51:2167–9.

[17] Saletti R, Neri B, Olivo P, Modelli A. Correlated fluctuations and noise spectra of tunneling and substrate currents before breakdown in thin-oxide MOS devices. IEEE Trans Electron Dev 1990;37:2411–3.

[18] Alers GB, Krish KS, Monroe D, Weir BE, Chang AM. Tunneling current noise in thin gate oxides. Appl Phys Lett 1996;69(19):2885–7.

[19] Alers GB, Weir BE, Alam MA, Timp GL, Sorch T. Trap assisted tunneling as a mechanism of degradation and noise in 2–5 nm oxides. IRPS 1998:76–9.

[20] Riccò B, Gozzi G, Lanzoni M. Modeling and simulation of stress-induced leakage current in ultrathin SiO_2 films. IEEE Trans Electron Dev 1998;45(7):1554–60.
[21] Datta S. Electronic transport in mesoscopic systems. Cambridge: University Press; 1995.
[22] Lombardo S, Crupi F, La Magna A, Spinella C, Terras A, La Mantia A, et al. Electrical and thermal transient during dielectric breakdown of thin oxides in metal-SiO_2-silicon capacitors. J Appl Phys 1998;84(1): 472–9.